

CHEMISTRY

A European Journal



Accepted Article

Title: Reverse solvatochromism of imine dyes comprised of 5-nitrofuran-2-yl or 5-nitrothiophen-2-yl as electron acceptor and phenolate as electron donor

Authors: Carlos Eduardo Albino Melo, Celso Rodrigo Nicoleti, Marcos Caroli Rezende, Adailton João Bortoluzzi, Renata Silva Heying, Robson Silva Oliboni, Giovanni Finoto Caramori, and Vanderlei Gageiro Machado

This manuscript has been accepted after peer review and appears as an Accepted Article online prior to editing, proofing, and formal publication of the final Version of Record (VoR). This work is currently citable by using the Digital Object Identifier (DOI) given below. The VoR will be published online in Early View as soon as possible and may be different to this Accepted Article as a result of editing. Readers should obtain the VoR from the journal website shown below when it is published to ensure accuracy of information. The authors are responsible for the content of this Accepted Article.

To be cited as: *Chem. Eur. J.* 10.1002/chem.201800613

Link to VoR: <http://dx.doi.org/10.1002/chem.201800613>

Supported by
ACES

WILEY-VCH

Reverse solvatochromism of imine dyes comprised of 5-nitrofuran-2-yl or 5-nitrothiophen-2-yl as electron acceptor and phenolate as electron donor

Carlos E. A. de Melo,^[a] Celso R. Nicoleti,^[a] Marcos C. Rezende,^[b] Adailton J. Bortoluzzi,^[a] Renata da S. Heying,^[a] Robson da S. Oliboni,^[c] Giovanni F. Caramori,^[a] Vanderlei G. Machado*^[a]

Abstract: Eight compounds with phenols as electron-donating groups and 5-nitrothiophen-2-yl or 5-nitrofuran-2-yl acceptor moieties in their molecular structures were synthesized. The crystalline structures of six compounds were obtained. Their corresponding phenolate dyes were studied in 29 solvents and the data showed that in all cases a reverse solvatochromism occurred. The results were explained in terms of the ability of the medium to stabilize the electronic ground and excited states of the probes to different extents. The frontier molecular orbitals were analyzed for the protonated and deprotonated forms of the compounds. The calculated geometries are in agreement with X-ray structures determined for the compounds and it was verified that after their deprotonation an increase in the electron delocalization occurs. Radial distribution functions were calculated for the dyes in water and *n*-hexane to analyze different solvation patterns resulting from the interaction of the solvents with the dyes. Data obtained using the Catalán multiparameter equation revealed that the medium acidity is responsible for hypsochromic shifts, while the solvent basicity, polarizability, and dipolarity contributed to bathochromic shifts of the solvatochromic band of these dyes. Two model "hybrid cyanine" dyes were used in the design of simple experiments to demonstrate that the solvatochromic behavior of these dyes in solution can be tuned with careful consideration of the properties of the medium.

Introduction

Solvatochromic dyes have been used in recent decades as probes to measure the polarity of solvents.^[1] These compounds exhibit bands in the visible region and their position and/or intensity is dependent on the nature of the medium. The best known example of a solvatochromic dye is the Reichardt pyridinium-*N*-phenolate betaine **1** (Scheme 1), whose visible charge transfer (CT) solvatochromic band was the basis for the development of the widely employed $E_T(30)$ empirical polarity solvent scale.^[1a, 2, 3]

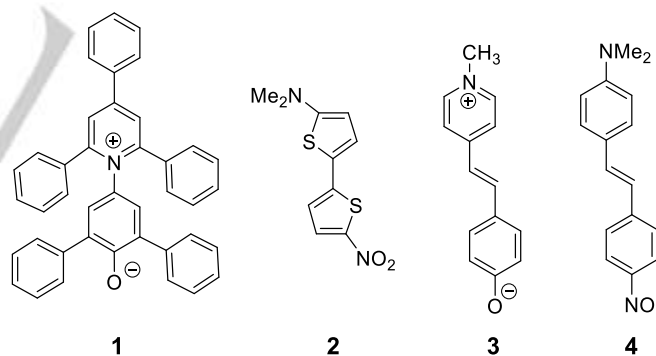
^[a] Departamento de Química, Universidade Federal de Santa Catarina, UFSC, CP 476, Florianópolis, SC, 88040-900, Brazil
E-mail: vanderlei.machado@ufsc.br

^[b] Facultad de Química y Biología, Universidad de Santiago, Av. B. O'Higgins 3363, Santiago, Chile

^[c] Centro de Ciências Químicas, Farmacêuticas e de Alimentos, Universidade Federal de Pelotas, UFPEL, Pelotas, RS, 96010-900, Brazil

Supporting information for this article can be found at <http://dx.doi.org/>

Compound **1** exhibits a negative solvatochromic behavior, meaning that the solvatochromic band of the probe is shifted toward a lower maximum wavelength (λ_{\max}) values when the polarity of the solvent is increased. The opposite behavior is found for compound **2**, introduced by Effenberger and coworkers.^[4] This compound is known for its very pronounced positive solvatochromism, with its vis solvatochromic band being displaced to increasing λ_{\max} values when the polarity of the medium is increased. It has also been verified that some families of solvatochromic dyes, for instance the classical Brooker's merocyanine (dye **3**)^[5] or compound **4**,^[6] interestingly present a reversal in their solvatochromic behavior. For these dyes, a negative solvatochromism is verified for the most polar solvents through to solvents exhibiting intermediate polarity, followed by a reversal in the solvatochromism, from negative to positive, occurring with a further reduction in the polarity of the solvent.



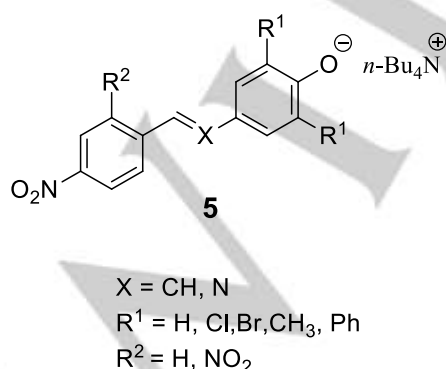
Scheme 1. Examples of class I and class II solvatochromic dyes.

Solvatochromic merocyanines (and other dyes with related molecular structures) are molecules composed of conjugated electron-donor and acceptor fragments, capable of an internal CT, which gives rise to a solvent-dependent transition. The relationship between this transition energy (E_T) and the nature of the two fragments can be rationalized with the aid of a *cyanine-limit model*.^[7] This model postulates a hyperbolic dependence of E_T on the solvatochromic strength (*S*) of the molecule, that is, the difference between the tendencies to donate and accept charge, by the donor and acceptor fragments, respectively. The model distinguishes two classes of merocyanines (or

merocyanine-like dyes): class I, constituted by charged donor and acceptor moieties, and class II, composed of two neutral fragments.^[8] Thus, solvatochromic dyes **1** and **3** are examples of class I, while compounds **2** and **4** are class II dyes. The two classes exhibit an opposite dependence of E_T on the S value of the molecule. The value of E_T increases with increased S for class I compounds, and decreases for class II dyes.

We have recently proposed a *generalized reversal model* for the interpretation of the behavior of solvatochromic dyes, as an alternative to the cyanine-limit model.^[9] Starting from the observation that the environment changes the solvatochromic strength of a dye, it is postulated that a minimum value of the transition energy should always exist for any merocyanine, as a consequence of the hyperbolic dependence of E_T on S. This minimum value is a point of solvatochromic reversal and thus all merocyanines should exhibit reverse or inverted solvatochromic behavior at some polarity value. This polarity value is frequently "virtual": if an extended polarity scale is employed, it occurs beyond the limits of the range of experimental solvent polarities, leading to the particular cases of a positive or a negative solvatochromism. "Real" reversal is verified only when this minimum occurs at some point within the range of experimental solvent polarities.^[9]

The emphasis put on the solvatochromic reversal of merocyanines naturally stimulates research on new dyes that exhibit a clear inverted behavior in solvents of medium polarity. We have been interested in a particular family of dyes of general structure **5** (Scheme 2),^[10, 11] with a phenolate donor conjugated with a polynitroaryl acceptor moiety, which, besides being readily accessible, satisfy the above requirement and also the need for good solvent sensitivity.

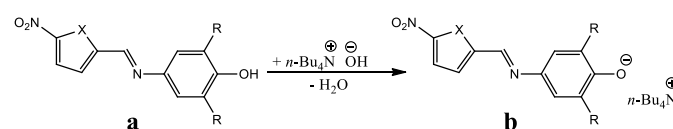


Scheme 2. General structure of a "hybrid cyanine" dye **5** with a phenolate donor and polynitrophenyl acceptor fragments.

We have termed these compounds "hybrid cyanine" dyes, as their molecular structure may be considered a hybrid of class I and class II dyes.^[10c] As a consequence, solvatochromic plots employing a class I dye as a reference, like the commonly employed $E_T(30)$ scale based on pyridinium *N*-phenolate betaine **1**, or a class II dye, such as probe **2**, inevitably yield poor correlations with the solvatochromic shifts of these "hybrid" compounds. We have therefore proposed the reference "hybrid" dye **5** (X = CH, R¹ = R² = H) to evaluate the effect of different structural features on the solvatochromic behavior of this family of compounds. E_T values for all of these derivatives correlate linearly with the E_T^{ref} values of the unsubstituted reference stilbene, in around 30 solvents with widely different polarities.^[10c] The simple two-parameter Eqn (1) yields values for the slope n and intercept m for any derivative **5**, thus allowing a quantitative comparison of these compounds, and revealing the effect of the variables R¹, R² and X on their solvatochromic behavior.

$$E_T = m + nE_T^{\text{ref}} \quad \text{Eqn (1)}$$

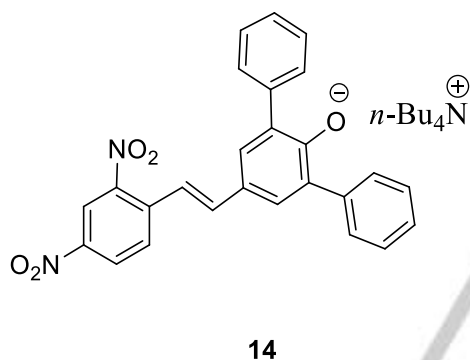
Searching for more sensitive derivatives in this family, we decided to prepare novel solvatochromic dyes by replacing the homoaromatic acceptor fragment with heterocyclic analogs (5-nitrothiophen-2-yl or 5-nitrofuran-2-yl groups). Compounds **6a–13a** (Scheme 3) were completely characterized and the crystalline structures of six compounds are presented. Like their homoaromatic analogs **5**, all of these phenolate dyes were generated *in situ* through the treatment of their phenolic precursors **6a–13a** with tetra-*n*-butylammonium hydroxide (TBAOH). Their solvatochromic behavior was studied in 29 solvents and compared with that of their homoaromatic analogs, with the aid of Eqn (1).



	6a,b	7a,b	8a,b	9a,b	10a,b	11a,b	12a,b	13a,b
X	S	S	S	S	O	O	O	O
R	H	CH ₃	Cl	Br	H	CH ₃	Cl	Br

Scheme 3. Compounds **6a–13a** and their deprotonation to generate **6b–13b**.

Besides rationalizing their solvatochromism by characterizing their internal charge–transfer in terms of their frontier molecular orbitals, the solvation of these dyes in water and in *n*-hexane was investigated by molecular simulations with two model cyanine–like dyes (compounds **6b** and **10b**). Multiparametric regression analysis allowed a comparison of the effect of specific solvent properties on their solvatochromic behavior. The trends observed were confirmed experimentally by studying the spectral response of some dyes, **6b** and **14**^[10c] (Scheme 4), to specific environmental changes (using an organic solvent like dichloromethane), brought about by the addition of a co–solvent or of a cationic species. Thus, besides their full characterization, these novel compounds provided additional experimental and theoretical information that helped us to understand and rationalize the solvatochromic inversion of this interesting family of “hybrid cyanine” dyes.

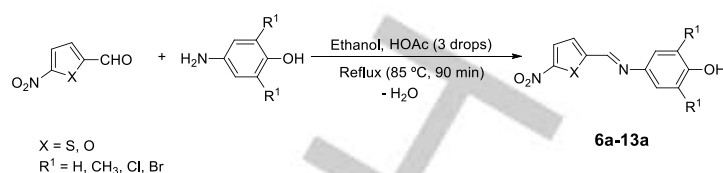


Scheme 4. Molecular structure of model “hybrid cyanine” solvatochromic dye **14**.

Results and Discussion

Synthesis of the compounds

The synthesis of compounds **6a–13a** was performed as shown in Scheme 5, using a methodology described by Stock et al.,^[10c] through the condensation of 5–nitro–2–thiophenecarboxyaldehyde or 5–nitro–2–furaldehyde with the corresponding aniline in the presence of acetic acid as the catalyst and ethanol as the solvent. The 2,6–substituted aminophenols were prepared according to a methodology described by Johnson et al.^[12] No purification technique was required for any of the compounds. The products of the reactions were obtained in yields of 50–88%. Compounds **7a**, **8a**, **9a**, **10a**, **11a**, **12a**, and **13a** are novel compounds and were characterized using IR, ¹H NMR, ¹³C NMR, HRMS, and DSC techniques (Figures S1–S40 in Supporting Information).



Scheme 5. Formation of compounds **6a–13a** by condensation of 5–nitro–2–thiophenecarboxyaldehyde or 5–nitro–2–furaldehyde with anilines.

The X–ray structure of compounds **6a**, **7a**, **9a**, **10a**, **12a**, and **13a**

Monocrystals of compounds **6a**, **7a**, **9a**, **10a**, **12a**, and **13a** were obtained, allowing their structural characterization through X–ray diffraction (Figure 1). Compounds **6a**, **9a**, **10a**, **12a**, and **13a** crystallize in the monoclinic system (space groups *P*–2₁/*n* for **6a**, **10a**, **12a**, and **13a** and *Cc* for **9a**) while compound **7a** crystallizes in the triclinic mode (space groups *P* $\bar{1}$). The main bond distances and torsion angles for the compounds are reported in Tables S1–S17 (Supporting Information). The crystallographic data show that the iminophenols have an (*E*)–configuration.

Figure 2 reproduces supramolecular crystalline arrays for compounds **12a** and **13a**. In these arrays, a single water molecule interacts through hydrogen–bonds with both the 2–nitrofuryl ring (2–nitro substituent and the oxygen of the furyl group) of one molecule and the phenolic hydroxyl group of another, binding together the molecules of the furyliminophenol. The fact that these supramolecular arrays mediated by water molecules occur only with compounds **12a** and **13a** (of the compounds analyzed) shows that this is a result of the combination of two features in the same molecule, i.e., the presence of (a) oxygen as a heteroatom, providing an atom able to act as a hydrogen–bonding acceptor species, and (b) halogen groups, which makes the hydroxyl in the phenolic moiety sufficiently acidic to act as a strong hydrogen–bonding donor group.

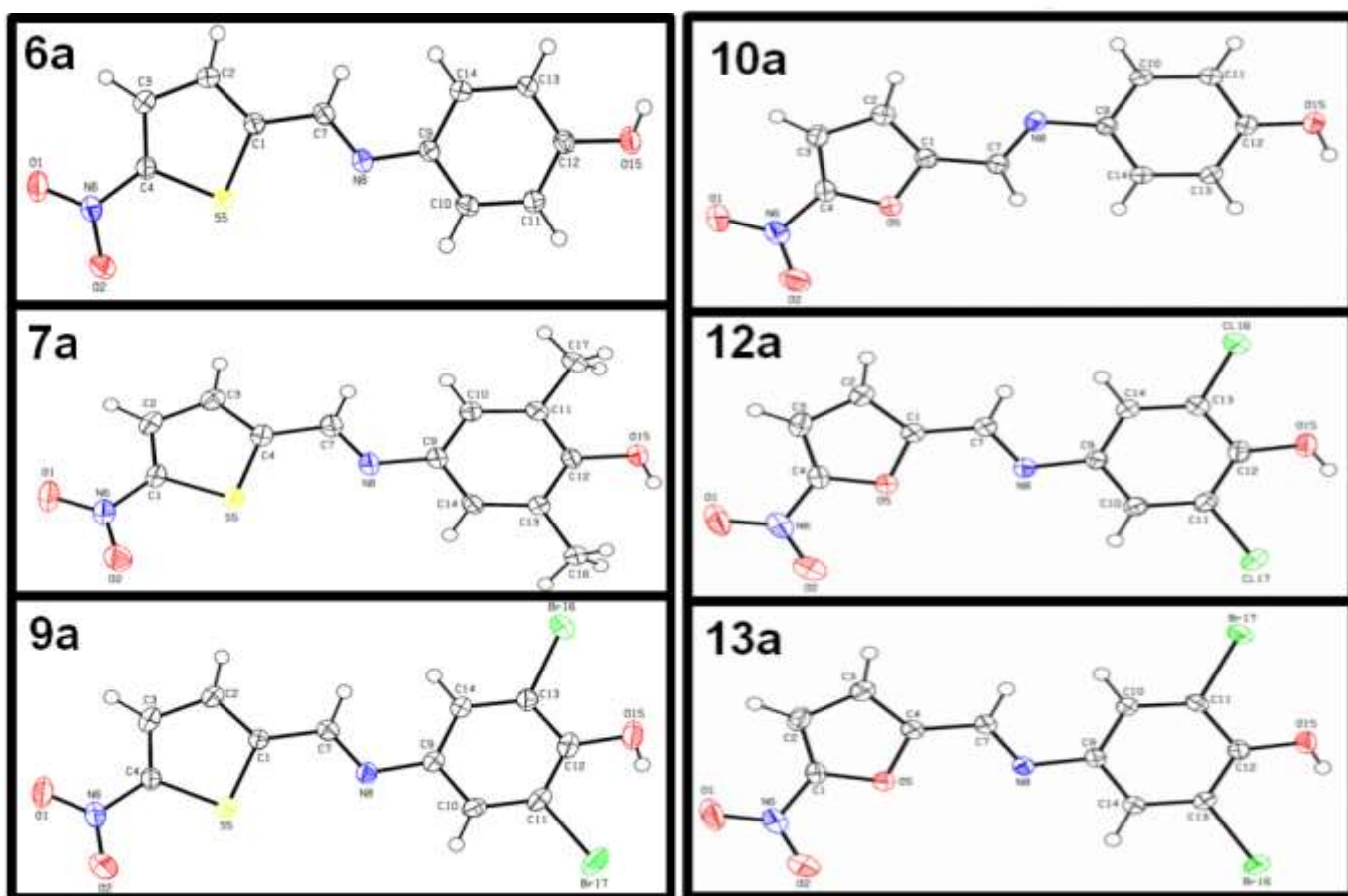


Figure 1. ORTEP projections of iminophenols **6a**, **7a**, **9a**, **10a**, **12a**, and **13a**.

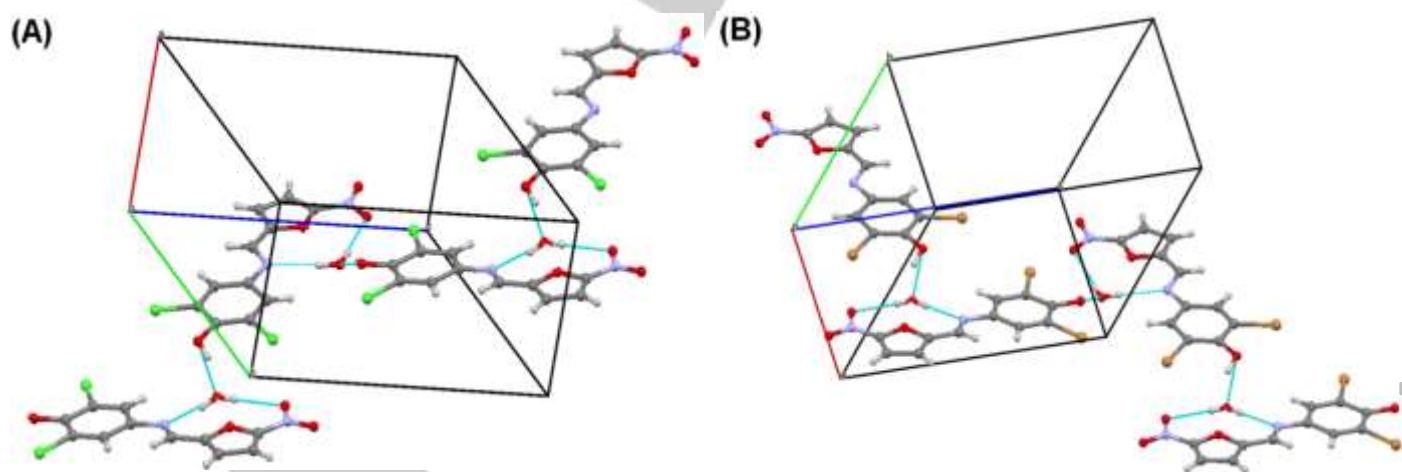


Figure 2. Supramolecular arrays of **12a** (A) and **13a** (B) crystals, with the inclusion of water molecules hydrogen-bonding with both the phenolic hydroxyl and the nitro substituents.

Table 1 lists, for all compounds, the C=N bond distances and dihedral angles between the phenolic and the 2-nitrothienyl or 2-nitrofuryl rings, as well as between the ring and the 2-nitro substituent. The length of the C=N bond in compounds **6a**, **7a**, and **9a** (with a 2-nitrothienyl ring) had a mean value of 1.276 Å while for compounds **10a**, **12a**, and **13a** (with a 2-nitrofuryl ring) a mean value of 1.281 Å was obtained.

Table 1. Some structural features of iminophenols **6a**, **7a**, **9a**, **10a**, **12a**, and **13a**.

Compound	Dihedral angle α (°) ^[a]	Dihedral angle β (°) ^[b]	C=N bond distance (Å)
6a	2.09	1.68	1.2763(12)
7a	4.25	1.38	1.2759(14)
9a	6.57	3.72	1.2750(3)
10a	10.08	11.15	1.2830(12)
12a	3.55	3.04	1.2790(16)
13a	3.41	2.49	1.2810(2)

[a] Dihedral angle between the phenolic and the 2-nitrothienyl or 2-nitrofuryl rings. [b] Dihedral angle between the heterocyclic ring and the 2-nitro group.

Nearly complete coplanarity between the phenolic ring and the nitro-substituted heterocyclic fragment was verified for all compounds, with small dihedral angles between the two rings (α) or between the heterocyclic ring and the nitro substituent (β). The dihedral angles for compound **10a** were slightly larger than the corresponding angles for the other iminophenols. Inspection of the ORTEP projections of **Figure 1** suggests that this difference might be due to the fact that **10a** crystallized with a conformation that differed from that of all other analogs.

Solvatochromic behavior of dyes **6b–13b**

Solutions of **6a–13a** are yellow, but after deprotonation using very small aliquots of TBAOH dyes **6b–13b** are generated, which exhibit different colors (**Figure 3A** and **Figure S41**). **Figure 3B** and **Figure S42** show the UV-vis spectra for dyes **6b–13b** in some selected solvents, confirming that the compounds are solvatochromic species. For instance, dye **11b** in water exhibits an absorption band with a maximum at 503 nm. This band is shifted to $\lambda_{\max} = 735$ nm in dimethylacetamide while in dimethylsulfoxide, trichloromethane, and *n*-hexane the band maximum is displaced to 733, 620, and 510 nm, respectively. The solvatochromic bands in the vis region of the spectra are a result of $\pi-\pi^*$ electronic transitions, with an intramolecular CT from the electron-donor phenolate moiety towards the electron-acceptor 2-nitrothienyl or 2-nitrofuryl moiety.

Compounds **6b–13b** are salts that, in principle, could form ion pairs in solution, which would influence the absorption spectra for the dyes, especially in low polarity solvents. Some experiments were performed in order to verify this possibility (see **Figures S43** and **S44**). The results are similar to those obtained previously for a series of (nitrostyryl)phenolate solvatochromic dyes.^[10b] Therefore, based on these experiments, the possibility of the formation of ion pairs in non-polar media was discarded.

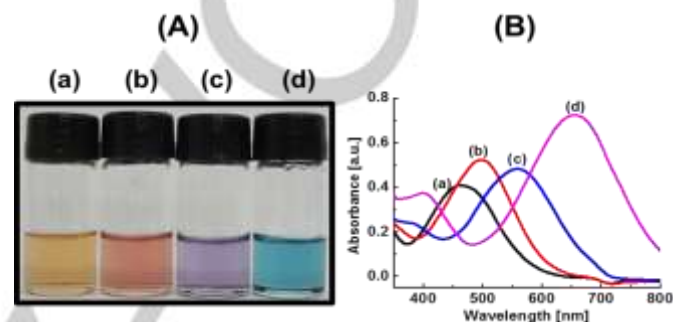


Figure 3. (A) Solutions and (B) UV-vis spectra for dye **10b** in (a) water, (b) methanol, (c) dimethoxyethane, and (d) acetone.

The spectra for dyes **6b–13b** were recorded in 29 solvents. The corresponding transition energies (E_T), in kcal mol⁻¹, are listed in **Table 2**. **Figure 4** shows a plot of the transition energies obtained as a function of the $E_T(30)$ solvent polarity values for dye **13b**, these being similar to those obtained for the other dyes (**Figure S45**). In all cases, an inverted behavior was observed, as previously described for analogous dyes **5**.^[10, 11] As a typical example, for dye **7b**, the solvatochromic band has a maximum at 573 nm [$E_T(7b) = 49.9$ kcal mol⁻¹] in *n*-hexane (the least polar solvent studied), while in DMSO $\lambda_{\max} = 798$ nm [$E_T(7b) = 35.8$ kcal mol⁻¹]. Thus, a reduction in the $E_T(7b)$ value occurs with an increase in the polarity of the medium, leading to a bathochromic shift of $\Delta\lambda_{\max} = +225$ nm, which is characteristic for a positive solvatochromism. The region of the plot corresponding to the solvent DMSO is where the reverse solvatochromism starts to occur. A further increase in the solvent polarity leads to an increase in the $E_T(7b)$ value, which is typical for a negative solvatochromism. The vis band of **7b** in water has a maximum at 519 nm [$E_T(7b) = 55.1$ kcal mol⁻¹], which, in comparison to the λ_{\max} value in DMSO, corresponds to a strong hypsochromic band shift of $\Delta\lambda_{\max} = -279$ nm.

Table 2. $E_T(30)$ and $E_T(\text{dye})$ values for compounds **6b**–**13b** in 29 solvents.

Solvent	$E_T(30)^{[a]}$	$E_T(6b)^{[b]}$	$E_T(7b)^{[b]}$	$E_T(8b)^{[b]}$	$E_T(9b)^{[b]}$	$E_T(10b)^{[b]}$	$E_T(11b)^{[b]}$	$E_T(12b)^{[b]}$	$E_T(13b)^{[b]}$
Cyclohexane	30.9	55.4	49.6	55.8	54.3	58.0	55.6	58.1	58.0
<i>n</i> -Hexane	31.0	56.5	49.9	56.8	56.2	58.5	56.0	58.4	58.5
Toluene	33.9	51.9	46.8	52.9	52.1	55.4	50.0	55.5	55.4
Ethyl ether	34.5	49.5	44.5	50.5	50.4	54.1	48.3	53.9	54.1
THF	37.4	46.0	39.6	47.7	47.0	49.1	43.8	51.4	50.9
Ethyl acetate	38.1	47.0	40.5	49.4	49.2	50.7	45.4	52.3	52.2
Dimethoxyethane	38.2	47.1	40.7	48.4	47.9	51.2	44.7	50.9	51.4
Trichloromethane	39.1	49.4	44.6	50.8	49.7	51.7	46.1	52.5	52.2
Acetophenone	40.6	47.1	41.4	46.4	45.8	49.9	43.1	49.3	49.3
Dichloromethane	40.7	48.4	42.5	50.1	49.2	51.0	45.2	52.1	51.4
1,2-Dichloroethane	41.3	48.3	42.4	50.1	49.1	51.2	45.1	51.8	51.6
Acetone	42.2	45.0	39.1	49.0	46.8	48.6	42.7	50.5	50.6
DMA	42.9	44.5	38.3	44.2	44.6	43.5	38.9	47.7	48.1
DMF	43.2	41.4	36.3	45.7	45.8	44.6	39.6	48.6	48.9
2-Methylpropan-2-ol	43.3	47.3	42.3	50.2	50.1	52.7	44.9	52.8	53.4
DMSO	45.1	40.8	35.8	45.5	45.9	43.7	39.0	48.7	48.8
Acetonitrile	45.6	47.0	41.2	49.5	49.1	49.7	43.7	52.0	51.9
Butan-2-ol	47.1	49.7	43.6	50.6	50.6	52.7	46.4	53.7	53.7
Decan-1-ol	47.7	52.7	47.1	53.6	53.0	55.9	50.0	56.1	56.0
Octan-1-ol	48.1	51.4	46.2	52.9	52.3	54.6	48.8	55.5	55.1
Propan-2-ol	48.4	50.9	44.8	51.5	51.6	54.2	47.9	54.7	54.7
Pentan-1-ol	49.1	52.6	47.0	53.4	52.9	56.1	49.8	56.1	55.8
Butan-1-ol	49.7	52.8	46.8	54.0	53.1	56.2	50.0	56.1	55.9
Benzyl alcohol	50.4	52.7	46.5	53.7	52.4	55.7	49.1	55.8	55.4
Propan-1-ol	50.7	53.6	47.6	54.0	53.9	56.7	50.5	56.8	56.5
Ethanol	51.9	54.5	48.4	55.5	54.6	57.3	51.3	57.3	57.3
Methanol	55.4	57.9	51.6	58.0	57.0	60.1	55.5	60.4	59.8
Ethane-1,2-diol	56.3	57.3	51.4	57.5	57.1	61.4	56.1	59.9	59.9
Water	63.1	58.9	55.1	60.3	60.0	61.6	56.9	62.5	62.2

[a] Values obtained from Reichardt.^[18] [b] In kcal mol⁻¹.

If a given 2-nitrothienyl dye is compared to its analogous 2-nitrofuryl dye (for instance **6b** with **10b**, **7b** with **11b**, and so on) the solvatochromism is more expressive for the thiophenyl dyes. In addition, in the same comparison, the λ_{max} values for the thiophenyl dyes are higher, suggesting that sulfur as a heteroatom facilitates the CT electronic transition. With respect to the substituents in the phenolate moiety, the strongest solvatochromic behavior occurs with the methyl group, which

increases the electronic density in the electron-donating moiety of the dye, increasing the probability of the occurrence of CT. On the other hand, the presence of chlorine or bromine as substituents causes the opposite effect, lowering the efficiency of the CT and resulting in a relatively weak solvatochromic behavior.

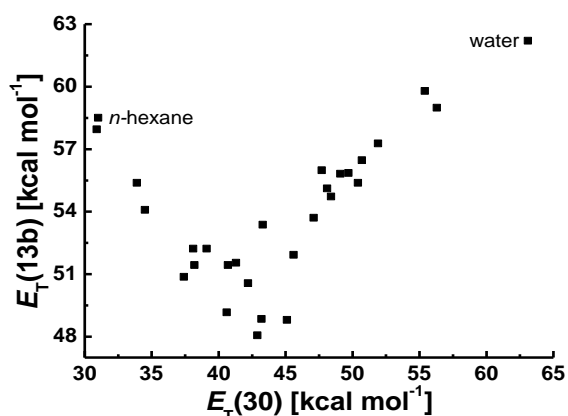


Figure 4. $E_T(30)$ value as a function of $E_T(\text{dye})$ for dye 13b.

Table 3. Values of λ_{max} for compounds 6b–13b in the most polar, least polar and intermediate polarity solvents, and the $\Delta\lambda_{\text{max}}$ values obtained considering the regions of positive and negative solvatochromism.

Dye	Most polar solvent (water) λ_{max} (nm)	Intermediate solvent λ_{max} (nm)	Least polar solvent (n-hexane) λ_{max} (nm)	$\Delta\lambda_{\text{max}}^{\text{[a]}}$ (nm)	$\Delta\lambda_{\text{max}}^{\text{[b]}}$ (nm)
6b	485	702 (DMSO)	506	+196	-221
7b	519	798 (DMSO)	573	+225	-279
8b	474	647 (DMA)	503	+144	-173
9b	476	641 (DMA)	509	+132	-165
10b	464	657 (DMA)	489	+168	-193
11b	503	735 (DMA)	510	+225	-232
12b	457	599 (DMA)	490	+109	-142
13b	460	595 (DMA)	489	+106	-135

[a] $\Delta\lambda_{\text{max}} = \lambda_{\text{max}}(\text{intermediate solvent}) - \lambda_{\text{max}}(n\text{-hexane})$.

[b] $\Delta\lambda_{\text{max}} = \lambda_{\text{max}}(\text{water}) - \lambda_{\text{max}}(\text{intermediate solvent})$.

A comparison of the heteroaromatic dyes 6b–13b with their homoaromatic analogs 5 could be made with the aid of Eqn (1). The intercept m in this equation is a measure of the average shift of the solvatochromic λ_{max} value for a given dye with respect to the stilbene reference 5 ($X = \text{CH}$, $R^1 = R^2 = \text{H}$) of Scheme 2. The slope n compares the solvatochromic sensitivity of the dye to polarity changes, with that of the same stilbene reference. Table 4 summarizes these values for dyes 6b–13b (Figure S46). In all cases, the linear correlations were good. Dyes with electron-donating substituents on the phenolate moiety had negative m values, indicating bathochromic shifts in their solvatochromic band with respect to the stilbene reference. Electron-accepting substituents, like Cl and Br in compounds 8b, 9b, 12b, and 13b, led to hypsochromic shifts in their solvatochromic band with respect to the same reference. They

also reduced the dye sensitivity to the medium polarity, with lower n values.

Table 4. Values for the slope n and intercept m in linear plots of $E_T(\text{dye})$ as a function of $E_T(5)$ values, for compounds 6b–13b.

Dye	m	n	r^2
6b	-5.48 ± 2.60	0.94 ± 0.04	0.94
7b	-11.55 ± 2.93	0.95 ± 0.05	0.93
8b	4.81 ± 2.64	0.79 ± 0.04	0.92
9b	6.32 ± 2.80	0.76 ± 0.04	0.90
10b	-4.43 ± 2.30	0.98 ± 0.04	0.96
11b	-13.37 ± 2.60	1.03 ± 0.04	0.95
12b	10.02 ± 2.35	0.75 ± 0.04	0.92
13b	11.47 ± 2.42	0.72 ± 0.04	0.91

Theoretical calculations

The frontier molecular orbital plots for 6a–6b and 10a–10b as well as their eigenvalues and HOMO–LUMO gaps indicate that, after deprotonation, the electron density delocalization increases significantly, as revealed by the decrease in the HOMO–LUMO gap (Figure 5).

In order to investigate the solvation of the dyes, molecular dynamics simulations of compounds 6b and 10b were performed with water and n-hexane as solvents. These two dyes were chosen as prototypes to analyze different solvation patterns that can arise depending on the acceptor group, and also to investigate the behavior of two solvents that are at the extremes of the solvatochromic scale. Radial distribution functions (RDFs) were calculated from equilibrated trajectories generated for the combination of the two dyes and solvents. The analysis was focused on the phenolate and nitro substituents of the donor and acceptor groups, respectively, on the nitrogen atom of the imino bridge, and on the furyl and thienyl rings in the compounds.

The two dyes yielded very similar RDFs around the phenolate oxygen (Figure 6A) with a first solvation shell centered at 1.8 Å with one water molecule, and a second more diffuse shell at 3.2 Å with four water molecules (Figure 7). The nitro oxygens of 6b and 10b also formed hydrogen bonds with the solvent, as shown by the RDFs of Figure 6B, giving rise to a first solvation shell centered at 2.1 Å with one water molecule. In addition, a second solvation shell, less intense as compared to the donor group, at 3.5 Å can be identified. A solvation shell is also verified around the nitro group, but this is less intense compared to the donor group. The heteroatoms of the thienyl

(compound **6b**) and furyl (compound **10b**) rings of the two dyes also showed a small, specific interaction with the surrounding water molecules, as indicated by the corresponding RDFs of **Figure 6C**, with small, diffuse solvation shells centered at 3.1 Å around the sulfur atom of **6b**, and at 2.5 Å around the furyl oxygen atom of **10b**. The shorter distance obtained for compound **11b** (O—HW) may be due to the more electronegative heteroatom in the bridging group. Finally, the imino nitrogen atom of both dyes showed a first solvation shell

centered at 2.2 Å with one water molecule and a second shell at 3.5 Å with three water molecules (**Figure 6D**). The comparison of the solvation results for the two dyes with *n*-hexane (see **Figure S47**) reveals that the solvation patterns are very similar. The data show the hydrogens of *n*-hexane interacting more strongly with the electronegative atoms of the dyes for both compounds. However, as would be expected, the interactions are much weaker than those verified in the intense and strongly packed first solvation shell with water.

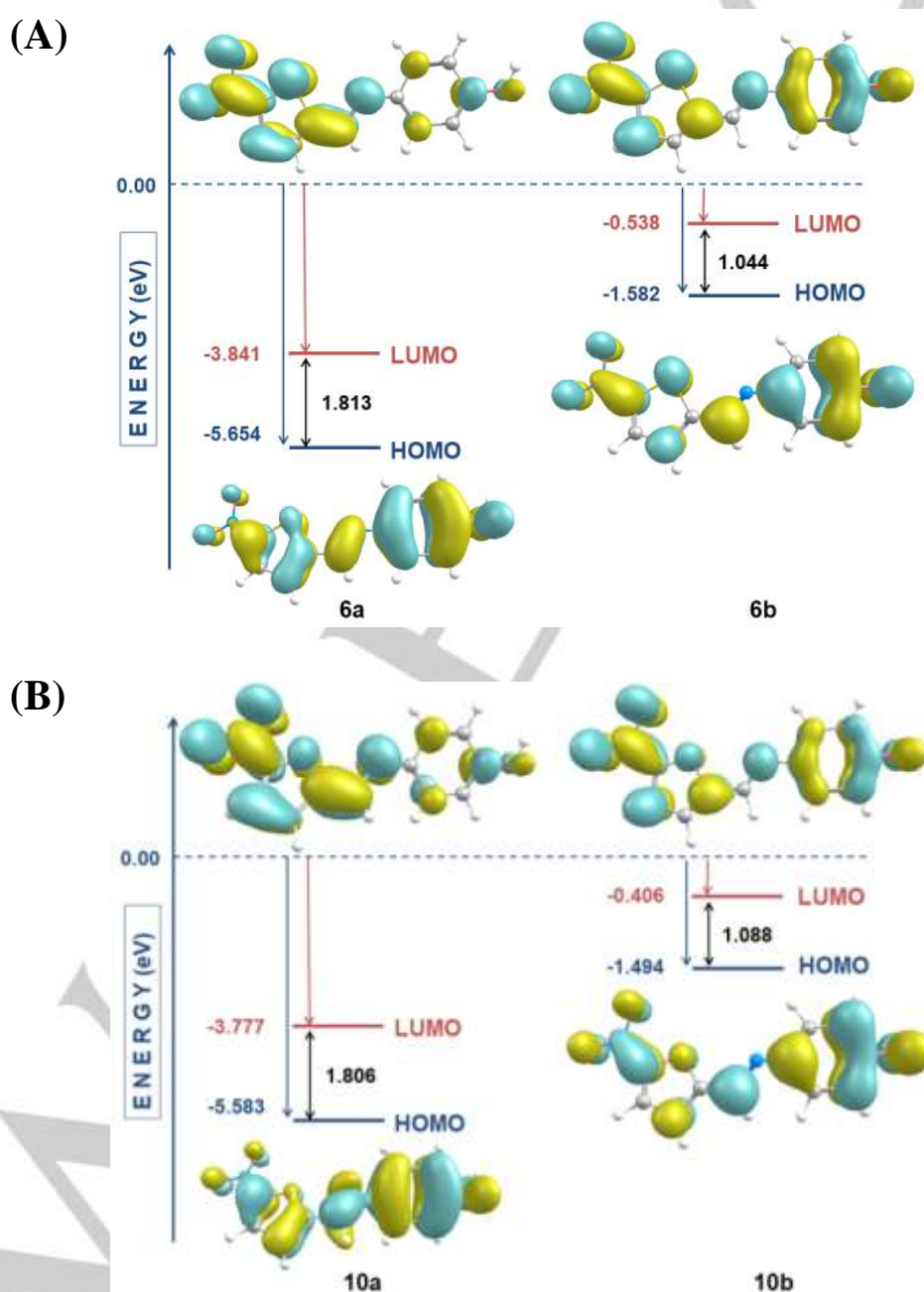


Figure 5. Contour plots and energies (eV) of the frontier orbitals (HOMO and LUMO) for compounds **(A) 6a, 6b** and **(B) 10a, 10b**.

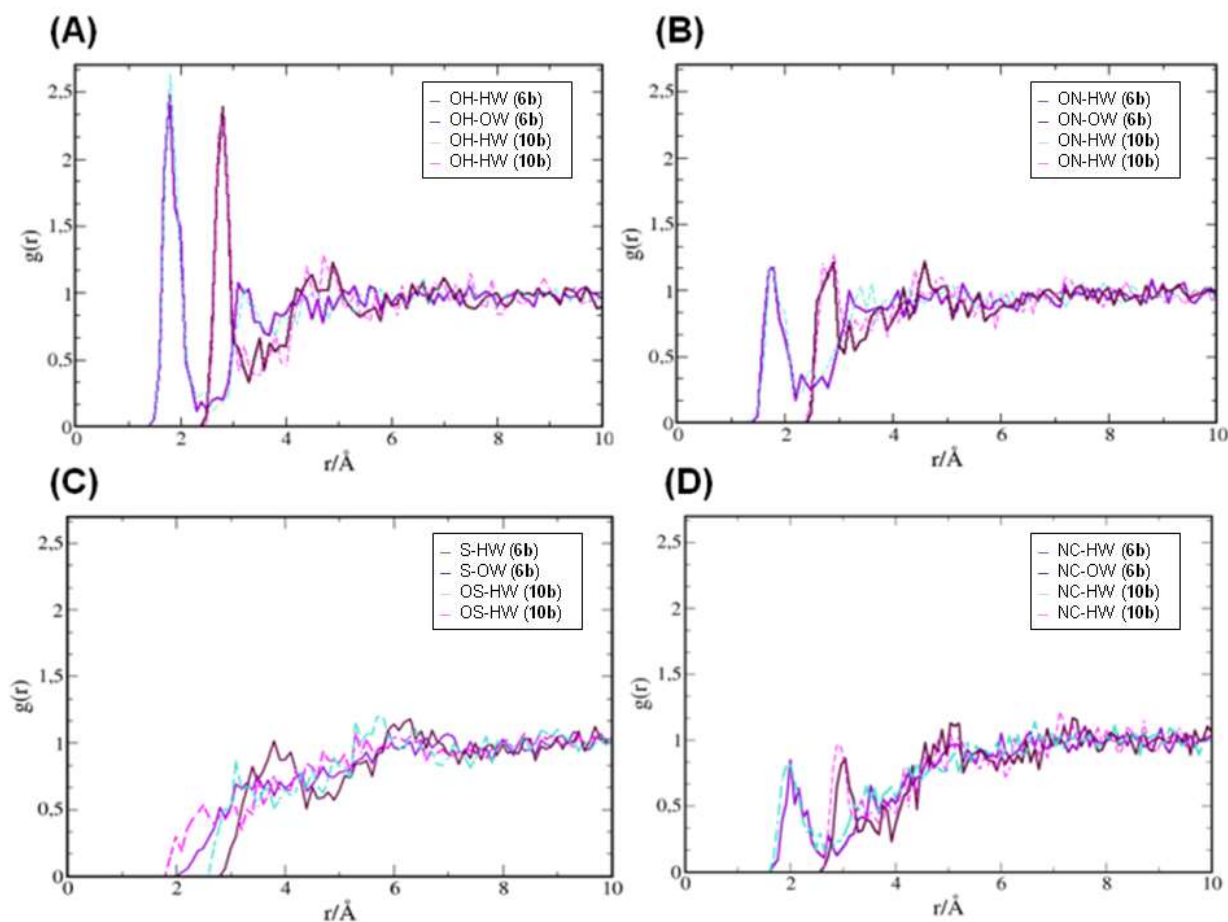


Figure 6. Radial distribution functions (RDFs) for the solvation of (A) phenolate oxygen, (B) nitro oxygens, (C) heteroatoms of the thienyl and furyl rings and (D) imino nitrogen bridge of **6b** and **10b** in water. A similar pattern was verified for the second oxygen of the nitro group. Atom types (HW) and (OW) denote the hydrogen and oxygen atoms of water, respectively, (OH) the oxygen of the phenolate group, (ON) the oxygen of the acceptor nitro group, and (NC) the nitrogen of the imino bridge, while (S) and (OS) represent the heteroatoms of thienyl and furyl rings of dyes **6b** and **10b**, respectively.

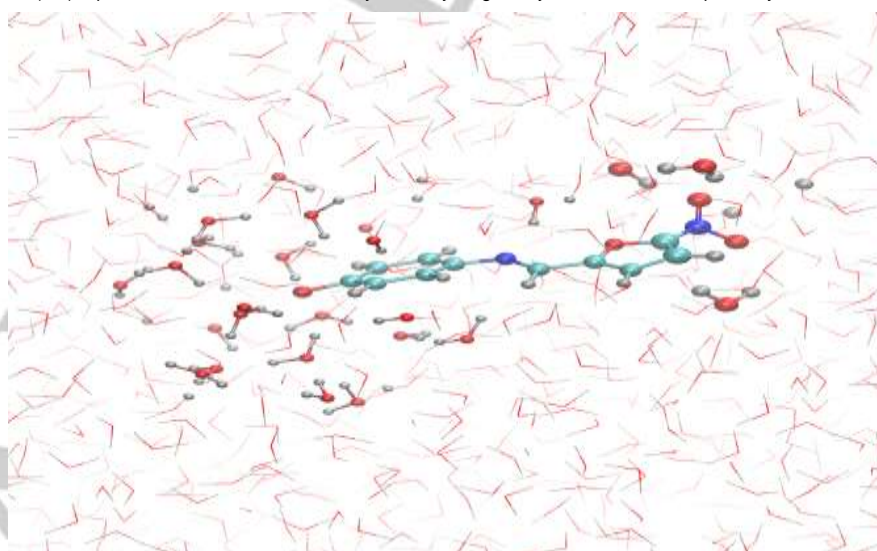


Figure 7. Snapshots of the molecular dynamics simulation emphasizing the two solvation shells of water molecules around **10b**. The water molecules highlighted are 6 Å from the oxygen of the phenolate group, and within 3 Å of the other groups.

Multiparametric regression analysis

The data in **Table 2** were subjected to a multiparametric regression analysis, according to Eqn (2), to compare the effects of different solvent properties, like acidity (*SA*), basicity (*SB*), dipolarity (*SdP*) and polarizability (*SP*), on the transition energies of dyes **6b–13b**.

$$E_T(\text{dye}) = E_T(\text{dye})_0 + aSA + bSB + cSP + dSdP \quad \text{Eqn (2)}$$

The Catalán parameters^[13] have proved to be superior to the Kamlet–Abboud–Taft parameters^[13a, 14] in previous regressions with hybrid dyes **5**.^[10] In general, the exclusion of

data points obtained in water from the regressions led to improved correlations. **Table 5** lists the values for the coefficients *a*, *b*, *c*, and *d*, obtained for dyes **6b–13b**. As verified for dyes **5** (**Scheme 2**),^[10] the medium acidity was responsible for hypsochromic shifts in the solvatochromic band of the heteroaromatic analogs **6b–13b**, with positive values for coefficient *a*. In contrast, the solvent basicity, polarizability, and dipolarity, all with negative values for the corresponding coefficients, contributed to a decrease in the transition energies, or to bathochromic shifts in the solvatochromic band of these dyes.

Table 5. Correlation coefficients *a*, *b*, *c*, and *d* obtained from the Catalán multiparametric (Eqn 2) analysis through the treatment of $E_T(\text{dye})$ values for compounds **6b–13b** in various solvents.

Dye	$E_T(\text{dye})_0$	<i>a</i>	<i>b</i>	<i>c</i>	<i>d</i>	<i>N</i> ^[a]	<i>R</i> ^[b]	S.D. ^[c]
6b	61.94	16.28	-3.11	-9.02	-10.14	29	0.95	1.58
6b ^[d]	64.70	20.87	-5.94	-12.47	-9.28	28	0.98	0.93
7b	55.09	17.03	-3.42	-7.48	-10.48	29	0.97	1.24
7b ^[d]	57.07	20.33	-5.45	-9.96	-9.46	28	0.98	0.84
8b	63.43	14.09	-3.10	-10.79	-7.80	29	0.96	1.12
8b ^[d]	65.42	17.40	-5.14	-13.27	-7.18	28	0.98	0.64
9b	62.19	13.90	-2.40	-10.85	-7.25	29	0.97	0.92
9b ^[d]	63.76	16.51	-4.00	-12.81	-6.76	28	0.99	0.57
10b	65.35	16.71	-2.49	-9.48	-10.93	29	0.94	1.68
10b ^[d]	68.19	21.43	-5.40	-13.02	-10.05	28	0.98	1.05
11b	63.52	17.00	-3.91	-12.42	-12.23	29	0.96	1.37
11b ^[d]	66.25	21.54	-6.71	-15.83	-11.38	28	0.99	0.51
12b	64.72	13.56	-2.09	-9.89	-7.55	29	0.97	0.85
12b ^[d]	66.29	16.17	-3.70	-11.85	-7.07	28	0.99	0.45
13b	65.51	12.75	-1.91	-11.33	-7.30	29	0.98	0.74
13b ^[d]	66.76	14.83	-3.20	-12.90	-6.91	28	0.99	0.46

[a] Number of solvents. [b] Linear correlation. [c] Standard deviation. [d] Excluding water from the studies.

Analysis of the influence of the solvent properties on the reverse solvatochromism of the dyes

As discussed in the previous section, medium acidity on the one hand and solvent basicity, polarizability and dipolarity on the other hand represent opposite trends which are responsible for the minima verified in all plots of **Figure 4**, and are a consequence of the hybrid nature of these dyes. In order to highlight this through direct observation, we recorded the solvatochromic shifts of some of these compounds in solvent mixtures composed of two solvents or of a solvent and an electrolyte. The rationale behind these experiments is that, with the use of an appropriate “co-solvent”, a specific interaction can be varied in a solvent mixture without affecting significantly the other properties of the medium. The resulting solvatochromic

shifts of the dye in such media must then reflect variations in that specific interaction.

Compounds **6b** and **14**^[10c] were chosen as model “hybrid cyanine” solvatochromic dyes. Dichloromethane was chosen as a reference solvent, capable of mixing in all ratios with a more polar solvent and of solubilizing an organic electrolyte. Its acidity (*SA* = 0.040) and basicity (*SB* = 0.178) are negligible.^[13e] The polarizability (*SP* = 0.761) and dipolarity (*SdP* = 0.769) of this solvent are reasonably high, but still allow room for increased values of basicity and dipolarity, in mixtures with solvents like DMF (*SA* = 0.031, *SB* = 0.613, *SP* = 0.759, *SdP* = 0.977) or DMSO (*SA* = 0.072, *SB* = 0.647, *SP* = 0.830, *SdP* = 1.00).^[13e] Thus, binary solutions of CH₂Cl₂/DMF or of CH₂Cl₂/DMSO allow a controlled and specific increase in the dipolarity and basicity

values, as they become richer in the more polar component DMF or DMSO.

The addition of a soluble organic electrolyte like sodium tetraphenylborate (NaPh_4B) to dichloromethane or DMF should result in mixtures with negligible variations in basicity, dipolarity or polarizability, but with strongly increased acidity values. This results from the strong tendency of the sodium cation to associate with the phenolate anion of the model dyes. As an electrophile–donor “co–solvent”, NaPh_4B behaves as a hydrogen–bond donor, increasing the transition energy of the phenolate dye and blue–shifting its solvatochromic band.

Figure 8A shows the variations in the E_T value of dye **6b** in binary mixtures of $\text{CH}_2\text{Cl}_2/\text{DMF}$. In all cases, decreased transition energies result from the addition of the more dipolar and basic co–solvent. The opposite trend is verified when DMF is replaced by the polar NaPh_4B “co–solvent” (**Figure 8B**). Addition of this sodium salt to a solution of **6b** in dichloromethane leads to increased E_T values and hypsochromic shifts in the solvatochromic band of the dye.

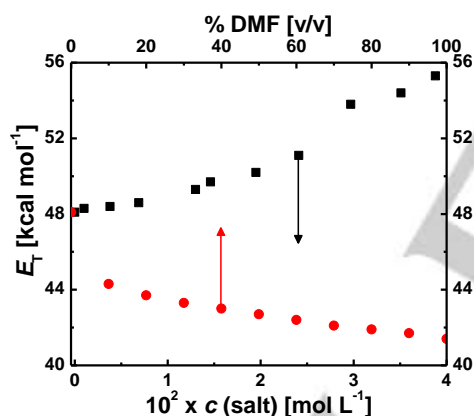


Figure 8. Opposite effects of the addition of a more polar “co–solvent” to solutions of the nitrothienyliminophenolate **6b** in CH_2Cl_2 : (A) bathochromic shift (transition–energy decrease) caused by addition of DMF (●); (B) hypsochromic shift (transition–energy increase) caused by addition of sodium tetraphenylborate (■).

The negative halochromic shifts caused by the sodium salt reflect the association of the phenolate dye with the Na^+ cation. Similar effects are verified in solutions of dye **14** (**Scheme 5**) in CH_2Cl_2 and in DMF. In both cases, the addition of increasing concentrations of NaPh_4B leads to increased E_T values for the solvatochromic band of the dye (**Figure 9**). NaPh_4B acts as a polar electrophile–bond–donor (EBD) “co–solvent”, increasing

the medium acidity, or its EBD strength, without affecting significantly its dipolarity or basicity.

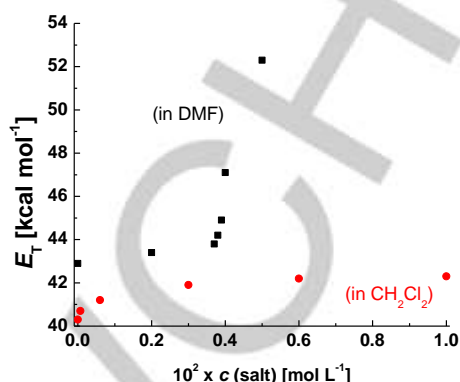


Figure 9. Variations in the E_T value of the solvatochromic band of dye **14** in (A) dichloromethane (●) and (B) DMF (■), through the addition of increasing concentrations of NaPh_4B .

Comparison of the plots for the solutions of **14** containing increasing concentrations of NaPh_4B in DMF and in CH_2Cl_2 (**Figure 9**) reveals a notable difference in the dye sensitivity to the addition of salt. The halochromism observed is more pronounced in DMF than in CH_2Cl_2 . This can be rationalized by the greater dissociation of the NaPh_4B salt in DMF than in CH_2Cl_2 , enhancing the availability of the sodium cation to associate with the phenolate dye. NaPh_4B in CH_2Cl_2 behaves as a covalent species, unable to affect the dye transition energy through cation complexation with the phenolate group. Much larger salt concentrations are thus required to induce halochromic shifts by the sodium salt.

The above arguments and evidences can be used to interpret the observed solvatochromic inversion of these “hybrid cyanine” dyes in solutions of medium polarity. In spite of their structural variations, this family of compounds exhibit a solvatochromic reversion in a narrow region of solvent polarities, characterized by intermediate E_T^N values (0.4–0.5).^[10,11] Minimum E_T values are verified with the same group of solvents, all of them showing negligible acidity, and significant dipolarity–polarizability and basicity. Medium acidity clearly increases the internal CT energy, by partially protonating the phenolate oxygen donor (in the case of hydrogen–bond donating solvents), or by reducing its charge through association with a cationic electrophile, as occurs with a “co–solvent” like NaPh_4B . Nevertheless, the CT energy also increases in non–polar, non–hydrogen–bond donating solvents, which have difficulty

promoting the phenol ionization necessary to generate a solvatochromic species, even in the presence of an added base (like TBAOH). Increasing the medium dipolarity–polarizability and, more importantly, the medium basicity, has the effect of increasing the effective charge on the phenolate oxygen, thus reducing the corresponding CT energy. This is evident from a comparison of the effect of two solvents with similar average values of dipolarity–polarizability, that is, dichloromethane ($SdP = 0.769$, $SP = 0.761$) and acetone ($SdP = 0.907$, $SP = 0.651$), but that differ appreciably in terms of basicity (SB values = 0.178 and 0.475 for dichloromethane and acetone, respectively).^[13e] The CT energies are consistently lower in acetone than in dichloromethane for all members of these “hybrid cyanine” dyes,^[10, 11] an observation that can be ascribed to the greater basicity of acetone. Increasing this basicity even further, using DMF, DMA or DMSO, leads in all cases to a consistent bathochromic shift of the solvatochromic band of these phenolate dyes. These shifts are readily explained by the reduction in the stability of the ground–state charged phenolate caused by a solvating, basic solvent. Internal CT and charge–dispersion are therefore promoted by such a solvent, leading to a more stabilized excited state.

Conclusions

Iminophenols **6a–13a**, which present heterocyclic (5–nitrothiophen–2–yl or 5–nitrofuran–2–yl) acceptor moieties in their molecular structures, were synthesized and characterized. Their deprotonation in solution led to the formation of their corresponding phenolate dyes **6b–13b**. The absorption band in the vis region of the spectra for each dye is related to a π – π^* electronic transition, of an intramolecular charge–transfer nature, from the electron–donor phenolate toward the electron–acceptor heterocyclic group. A study was performed in 29 different solvents, showing in all cases a reversal in solvatochromism. These “hybrid cyanine” dyes exhibit a solvatochromic behavior similar to that of their homoaromatic analogs,^[9, 10] with the solvatochromic reversion occurring in a narrow region of solvent polarities, characterized by intermediate E_T^N values (0.4–0.5).

The reverse solvatochromism of the dyes studied was discussed in the light of the fact that changes in the polarity of the solvent can modify the contribution weight of the quinonoid (less dipolar) and benzenoid (more dipolar) forms to the resonance hybrid of the dyes, causing changes in the energies

of the electronic ground and excited states of the dyes and, consequently, in the energy related to the charge–transfer electronic transition.

The frontier molecular orbitals were analyzed for the protonated and deprotonated forms of the compounds. The calculated geometries are in agreement with X–ray structures verified for the compounds studied, it being verified that an increase in the electron delocalization occurs for the phenolate dyes in comparison with their corresponding phenols. RDFs were calculated for the dyes in water, showing that although solvent molecules are found in the solvation shell of the dye around the phenolate oxygen, nitro oxygen, and imino nitrogen atoms, the most intense solvation is on the donor phenolate group. A study was also performed using *n*–hexane as the solvent. Although the solvation pattern is similar (hydrogens of *n*–hexane interact more strongly with the electronegative atoms of the compounds) the interactions are much weaker than those occurring with water as a solvent, due to the ability of the latter to form strong hydrogen bonds with the electronegative atoms of the dyes.

The Catalán multiparameter approach provided a good fit with the experimental data, showing that the medium acidity was responsible for hypsochromic shifts, while the solvent basicity, polarizability, and dipolarity contributed to the bathochromic shifts of the solvatochromic band of these dyes. These opposite contributions could be responsible for the reversal in the solvatochromism verified in these systems. In order to investigate this supposition, simple experiments were performed using the model “hybrid cyanine” solvatochromic dyes **6b** and **14**, based on the use of carefully chosen solvent mixtures or of a solvent and an electrolyte, so that a specific interaction could be varied in the system without affecting the other medium properties significantly. The experiments performed indicated that the solvatochromic behavior of these dyes in solution can be tuned with careful consideration regarding the properties of the medium.

Experimental Section

All reagents and solvents were analytically pure and they were purchased from commercial sources (Sigma–Aldrich and Vetec). The solvents were HPLC grade and were purified following the methodology described in the literature.^[15] Deionized water was used for all measurements and it was boiled and bubbled with

nitrogen and kept in a nitrogen atmosphere to avoid the presence of carbon dioxide. Dye **14** was obtained according with a previously described procedure.^[10c]

NMR spectra were recorded with 200 MHz Bruker AC-200F and with 400 MHz Bruker Avance 400 spectrometers. Chemical shifts were recorded in ppm with the solvent resonance as the internal standard and data are reported as follows: chemical shift, multiplicity (*s* = singlet, *d* = doublet), coupling constants (Hz), and integration. IR spectra were obtained with an FT Varian 3100 spectrometer, using KBr pellets. High-resolution mass spectra were collected using a Bruker OTOF-Q II 10243 equipment. UV-Vis spectra were obtained with an Agilent Technologies Cary 60 spectrometer. The melting points were determined by means of DSC analysis, using a Perkin Elmer Jade-DSC apparatus.

General procedure for the preparation of iminophenols. In a round-bottom flask, 5-nitro-2-thiophenecarboxyaldehyde or 5-nitro-2-furaldehyde (0.7 mmol), 1 equivalent of the corresponding amine, 3 mL of ethanol previously dried with molecular sieves (4 Å), and 3 drops of acetic acid were mixed together. The mixture was maintained under reflux at 85 °C for 90 min and the precipitate was then filtered and washed with ice-cold ethanol. No purification technique was required for any of the compounds.

(E)-4-(((5-nitrothiophen-2-yl)methylene)amino)phenol (6a).

This compound was prepared from 4-aminophenol and 5-nitro-2-thiophenecarboxyaldehyde as red crystals (yield: 82%). m.p.: 227.57 °C. [m.p. lit.^[16] = 219 – 220 °C]. IR (KBr, $\bar{\nu}_{\max}/\text{cm}^{-1}$): 3404 (OH); 1615 (C=N); 1570 and 1493 (N=O); 1203 (C-S). ¹H NMR (400 MHz, DMSO-*d*₆) δ /ppm: 9.80 (*s*, 1H); 8.84 (*s*, 1H); 8.14 (*d*, 1H, *J* = 4.0 Hz); 7.61 (*d*, 1H, *J* = 4.0 Hz); 7.29 (*d*, 2H, *J* = 8.4 Hz); 6.81 (*d*, 2H, *J* = 8.4 Hz). ¹³C NMR (100 MHz, DMSO-*d*₆) δ /ppm: 157.85; 151.61; 149.61; 149.00; 140.44; 130.42; 130.42; 130.32; 123.33; 115.85. HRMS *m/z*: 247.01722 [M-H]⁻, calculated for C₁₁H₇N₂O₃S, 247.01719.

(E)-2,6-dimethyl-4-(((5-nitrothiophen-2-yl)methylene)

amino)phenol (7a). This compound was prepared from 2,6-dimethyl-4-aminophenol and 5-nitro-2-thiophenecarboxyaldehyde as red crystals (yield: 65%). m.p.: 185.24 °C. IR (KBr, $\bar{\nu}_{\max}/\text{cm}^{-1}$): 3395 (OH); 2914 (C-H); 1599 (C=N); 1533 and 1482 (N=O); 1207 (C-S). ¹H NMR (200 MHz, acetone-*d*₆) δ /ppm: 8.82 (*s*, 1H); 8.04 (*d*, 1H, *J* = 4.3 Hz); 7.58 (*d*, 1H, *J* = 4.3 Hz); 7.08 (*d*, 2H, *J* = 0.7 Hz); 2.26 (*d*, 2H, *J* = 0.7 Hz). ¹³C NMR (100 MHz, DMSO-*d*₆) δ /ppm: 153.58; 151.54;

149.80; 148.84; 140.34; 130.38; 130.29; 124.99; 121.96; 16.51. HRMS *m/z*: 275.0488 [M-H]⁻, calculated for C₁₃H₁₁N₂O₃S, 275.0485.

(E)-2,6-dichloro-4-(((5-nitrothiophen-2-yl)methylene)

amino)phenol (8a). This compound was prepared from 2,6-dichloro-4-aminophenol and 5-nitro-2-thiophenecarboxyaldehyde as a yellow solid (yield: 50%). m.p.: 194.86 °C. IR (KBr, $\bar{\nu}_{\max}/\text{cm}^{-1}$): 3412 (OH); 1617 (C=N); 1533 and 1482 (N=O); 1205 (C-S); 1131 and 1034 (C-Cl). ¹H NMR (400 MHz, acetone-*d*₆) δ /ppm: 8.91 (*s*, 1H); 8.07 (*d*, 1H, *J* = 4.1 Hz); 7.68 (*d*, 1H, *J* = 4.1 Hz); 7.45 (*s*, 1H). ¹³C NMR (100 MHz, DMSO-*d*₆) δ /ppm: 152.91; 152.40; 148.87; 148.29; 141.27; 131.70; 130.23; 122.73; 122.17. HRMS *m/z*: 314.9393 [M-H]⁻, calculated for C₁₁H₅Cl₂N₂O₃S, 314.9392.

(E)-2,6-dibromo-4-(((5-nitrothiophen-2-yl)methylene)

amino)phenol (9a). This compound was prepared from 2,6-dibromo-4-aminophenol and 5-nitro-2-thiophenecarboxyaldehyde as dark yellow crystals (yield: 88%). m.p.: 219.51 °C. IR (KBr, $\bar{\nu}_{\max}/\text{cm}^{-1}$): 3487 (OH); 1607 (C=N); 1552 and 1497 (N=O); 1221 (C-S); 1042 (C-Br). ¹H NMR (400 MHz, acetone-*d*₆) δ /ppm: 8.90 (*s*, 1H); 8.07 (*d*, 1H, *J* = 4.3 Hz); 7.68 (*d*, 1H, *J* = 4.3 Hz); 7.64 (*s*, 1H). ¹³C NMR (100 MHz, DMSO-*d*₆) δ /ppm: 153.30; 152.40; 150.18; 148.17; 142.74; 131.82; 130.22; 125.69; 112.13. HRMS *m/z*: 404.8364 [M-H]⁻, calculated for C₁₁H₅Br₂N₂O₃S, 404.8362.

(E)-4-(((5-nitrofuran-2-yl)methylene)amino)phenol (10a).

This compound was prepared from 4-aminophenol and 5-nitro-2-furaldehyde as brown crystals (yield: 72%). m.p.: 183.60 °C (decomposes). IR (KBr, $\bar{\nu}_{\max}/\text{cm}^{-1}$): 3436 (OH); 1623 (C=N); 1580 and 1482 (N=O); 1272 (C-O). ¹H NMR (200 MHz, acetone-*d*₆) δ /ppm: 8.66 (*s*, 1H); 8.59 (*s*, 1H); 7.64 (*d*, 1H, *J* = 3.8 Hz); 7.38 (*d*, 2H, *J* = 8.8 Hz); 7.29 (*d*, 1H, *J* = 3.8 Hz); 6.93 (*d*, 2H, *J* = 8.8 Hz). ¹³C NMR (100 MHz, DMSO-*d*₆) δ /ppm: 157.84; 153.59; 152.02; 143.60; 140.99; 123.35; 116.42; 115.89; 114.38. HRMS *m/z*: 231.0402 [M-H]⁻, calculated for C₁₁H₇N₂O₄, 231.0400.

(E)-2,6-dimethyl-4-(((5-nitrofuran-2-yl)methylene)amino)

phenol (11a). This compound was prepared from 2,6-dimethyl-4-aminophenol and 5-nitro-2-furaldehyde as a dark red solid (yield: 65%). m.p.: 176.64 °C. IR (KBr, $\bar{\nu}_{\max}/\text{cm}^{-1}$): 3528 (OH); 2912 (C-H); 1578 (C=N) 1515 and 1488 (N=O); 1229 (C-O). ¹H NMR (200 MHz, acetone-*d*₆) δ /ppm: 8.60 (*s*, 1H); 8.56 (*s*, 1H); 7.79 (*d*, 1H, *J* = 3.9 Hz); 7.29 (*d*, 1H, *J* = 3.9 Hz); 7.09 (*s*, 1H); 2.18 (*s*, 6H). ¹³C NMR (100 MHz, DMSO-*d*₆) δ /ppm:

153.76; 153.65; 151.98; 143.43; 140.86; 124.98; 121.90; 116.33; 114.39; 16.62. HRMS m/z : 259.0716 $[M-H]^-$, calculated for $C_{13}H_{11}N_2O_4$, 259.0713.

(E)-2,6-dichloro-4-(((5-nitrofur-2-yl)methylene)amino)phenol (12a). This compound was prepared from 2,6-dichloro-4-aminophenol and 5-nitro-2-furaldehyde as brown crystals (yield: 84%). m.p.: 147.41 °C. IR (KBr, $\bar{\nu}_{max}/cm^{-1}$): 3595 (OH); 1650 (C=N); 1519 and 1495 (N=O); 1231 (C-O); 1180 and 1025 (C-Cl). 1H NMR (200 MHz, acetone- d_6) δ/ppm : 8.65 (s, 1H); 7.65 (d, 1H, $J = 3.8$ Hz); 7.48 (s, 1H); 7.38 (d, 1H, $J = 3.8$ Hz). ^{13}C NMR (100 MHz, DMSO- d_6) δ/ppm : 153.63; 153.35; 148.68; 147.70; 142.10; 122.73; 122.16; 118.11; 114.13. HRMS m/z : 298.9618 $[M-H]^-$, calculated for $C_{11}H_5Cl_2N_2O_4$, 298.9621.

(E)-2,6-dibromo-4-(((5-nitrofur-2-yl)methylene)amino)phenol (13a). This compound was prepared from 2,6-dibromo-4-aminophenol and 5-nitro-2-furaldehyde as dark yellow crystals (yield: 65%). m.p.: 155.90 °C. IR (KBr, $\bar{\nu}_{max}/cm^{-1}$): 3602 (OH); 1648 (C=N); 1515 and 1490 (N=O); 1229 (C-O); 1025 (C-Br). 1H NMR (200 MHz, acetone- d_6) δ/ppm : 8.66 (s, 1H); 7.80 (d, 1H, $J = 3.9$ Hz); 7.67 (s, 1H); 7.35 (d, 1H, $J = 3.9$ Hz). ^{13}C NMR (100 MHz, DMSO- d_6) δ/ppm : 152.59; 152.34; 150.39; 147.76; 143.25; 125.69; 118.15; 114.11; 112.25. HRMS m/z : 388.8594 $[M-H]^-$, calculated for $C_{11}H_5Br_2N_2O_4$, 388.8591.

UV-vis measurements. The following procedure was typical for all measurements performed. A stock solution of each compound (1.0×10^{-3} – 1.0×10^{-2} mol L^{-1}) was prepared in acetone. From this stock solution, 7–40 μL was transferred to 5-mL volumetric flasks. After evaporation of the acetone the compound was dissolved in the pure solvent, resulting in a solution presenting a final dye concentration of 2.0×10^{-5} – 5.0×10^{-5} mol L^{-1} . In order to generate the deprotonated compounds, 5–15 μL of a methanolic 0.1 mol L^{-1} TBAOH solution was added to each flask. The addition of this very small amount of methanol did not change the position of the UV-vis band of the dye. The bulky tetra- n -butylammonium ion has no influence on the UV-vis spectrum for the anionic dye. The UV-vis spectra were recorded at 25.0 °C. The maxima of the UV-vis spectra were calculated from the first derivative of the absorption spectrum, with a precision of ± 0.5 nm, and the reproducibility of the λ_{max} values was verified through the determination of two spectra for each dye in each pure solvent. The λ_{max} values thus obtained were transformed into $E_T(\text{dye})$ values, according to the expression $E_T(\text{dye}) = 28590/\lambda_{max}$,^[1] given in kcal mol^{-1} with a precision of ± 0.1 kcal mol^{-1} .

Calculation methods. The multiparametric analysis was performed from non-linear regressions using ORIGIN 8.5 software.

Single-crystal X-ray structure determinations. X-ray diffraction data were recorded on a Bruker APX-II DUO diffractometer equipped with an APEX II CCD area detector using graphite-monochromated Mo $K\alpha$ ($\lambda = 0.71073$ Å). The temperature was set at 200(2) K. The frames were recorded from ω and ϕ scans using APEX2^[17] and the integration procedure was performed using the SAINT and SADABS programs.^[17] The structures were solved and refined with SHELXS97 and SHELXL2013 software programs,^[18] respectively. All non-hydrogen atoms were refined anisotropically. Hydrogen atoms attached to C atoms were placed at their idealized positions using standard geometric criteria. Hydrogen atoms of the hydroxyl groups were located from the Fourier difference map and treated with riding model approximation. The ORTEP plots and partial packing diagram were drawn with PLATON^[19a] and MERCURY^[19b] software, respectively. Further crystallographic information is given in **Table 6**. Full tables containing the crystallographic data (except structural factors) have been deposited at the Cambridge Structural Database, as supplementary publication numbers CCDC 1813014–1813019. Copies of the data can be obtained free of charge at www.ccdc.cam.ac.uk.

Computational details. The molecular dynamics simulations were performed via the GROMACS package,^[20] using the OPLS-AA force field^[21] and the water model SPC/E.^[22] Simulation boxes containing the solvents (water and n -hexane) were thermalized at the NVT ensemble (temperature 298 K, $\tau = 0.1$ ps) for 500 ps and equilibrated at the NPT ensemble (pressure 1 bar, $\tau = 0.5$ ps) for 2 ns. To describe the anionic compounds via the molecular mechanics (MM) method, charges for the molecule were obtained via the CHelpG method^[23] using the Gaussian 09 package,^[24] at the DFT level of theory with the B3LYP functional^[25] and 6-31G** basis set.^[26]

Acknowledgements

The authors are grateful for the financial support of the Brazilian governmental agencies Conselho Nacional de Desenvolvimento Científico e Tecnológico (CNPq), Fundação de Amparo à Pesquisa e Inovação do Estado de Santa Catarina (FAPESC), Financiadora de Estudos e Projetos (FINEP), and Coordenação

de Aperfeiçoamento de Pessoal de Nível Superior (CAPES), as well as the Laboratório Central de Biologia Molecular (CEBIME/UFSC) and UFSC. M.C.R. also acknowledges Fondecyt (project 1140212, by Dicyt/USACH) and CNPq (PVE 2014, process 400322/2014–5).

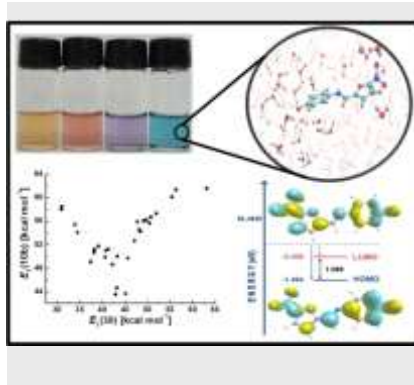
Keywords: solvatochromic dyes • solvatochromic reversal • solvatochromism • solute–solvent interactions

Table 6. Crystal data for compounds **6a**, **7a**, **9a**, **10a**, **12a**, and **13a**.

Compound	6a	7a	9a	10a	12a	13a
Empirical formula	C ₁₁ H ₈ N ₂ O ₃ S	C ₁₃ H ₁₂ N ₂ O ₃ S	C ₁₁ H ₆ Br ₂ N ₂ O ₃ S	C ₁₁ H ₈ N ₂ O ₄	C ₁₁ H ₈ Cl ₂ N ₂ O ₅	C ₁₁ H ₈ Br ₂ N ₂ O ₅
Formula weight	248.25	276.31	406.06	232.19	319.09	408.01
Temperature/K	200(2)	200(2)	200(2)	200(2)	200(2)	200(2)
Wavelength/Å	0.71073	0.7103	0.7103	0.71073	0.7103	0.7103
Crystal system	Monoclinic	Triclinic	Monoclinic	Monoclinic	Monoclinic	Monoclinic
Space group	<i>P</i> 2 ₁ / <i>n</i>	<i>P</i> 1	<i>C</i> c	<i>P</i> 2 ₁ / <i>n</i>	<i>P</i> 2 ₁ / <i>n</i>	<i>P</i> 2 ₁ / <i>n</i>
<i>a</i>/Å	9.0148(4)	7.9214(5)	14.0802(13)	8.9143(4)	6.98180(10)	7.16070(10)
<i>b</i>/Å	9.8884(5)	7.9456(7)	13.3380(12)	9.9006(4)	13.9271(3)	14.0854(3)
<i>c</i>/Å	12.2217(6)	12.3506(7)	6.9691(6)	11.7516(5)	13.2089(3)	13.0554(3)
α/°	90°	72.086(2)°	90°	90°	90°	90°
β/°	102.9210(10)°	76.878(2)°	94.548(2)°	104.5550(10)°	92.9950(10)°	90.9230(10)°
γ/°	90°	60.1790(10)°	90°	90°	90°	90°
Volume/Å³	1061.88(9)	639.13(8)	1304.60(2)	1003.87(7)	1282.63(4)	1316.61(5)
Z	4	2	4	4	4	4
Density (calculated)/mg m⁻³	1.553	1.436	2.067	1.536	1.652	2.058
Absorption coefficient/mm⁻¹	0.301	0.258	6.377	0.120	0.527	6.177
F(000)	512	288	784	480	648	792
Crystal size/mm³	0.400 × 0.200 × 0.160	0.400 × 0.200 × 0.100	0.400 × 0.220 × 0.120	0.400 × 0.380 × 0.200	0.340 × 0.160 × 0.120	0.220 × 0.120 × 0.120
Theta range for data collection	2.677 to 32.787°	1.740 to 30.525°	2.106 to 33.232°	2.580 to 30.651°	2.126 to 30.133°	2.127 to 30.144°
Index ranges	-13 ≤ <i>h</i> ≤ 7 -15 ≤ <i>k</i> ≤ 15 -18 ≤ <i>l</i> ≤ 18	-11 ≤ <i>h</i> ≤ 11 -11 ≤ <i>k</i> ≤ 11 -17 ≤ <i>l</i> ≤ 17	-21 ≤ <i>h</i> ≤ 21 -20 ≤ <i>k</i> ≤ 20 -10 ≤ <i>l</i> ≤ 10	-11 ≤ <i>h</i> ≤ 12 -14 ≤ <i>k</i> ≤ 14 -16 ≤ <i>l</i> ≤ 13	-6 ≤ <i>h</i> ≤ 9 -19 ≤ <i>k</i> ≤ 18 -16 ≤ <i>l</i> ≤ 18	-10 ≤ <i>h</i> ≤ 6 -19 ≤ <i>k</i> ≤ 19 -18 ≤ <i>l</i> ≤ 18
Reflections collected	15027	24192	13904	10614	13748	15810
Independent reflections	3934 [R(int) = 0.0156]	3903 [R(int) = 0.0219]	4777 [R(int) = 0.0289]	3097 [R(int) = 0.0167]	3777 [R(int) = 0.0206]	3871 [R(int) = 0.0233]
Completeness to theta = 25.242°	99.9%	100.0%	100.0%	100.0%	100.0%	99.9%
Absorption correction	Semi-empirical from equivalents					
Refinement method	Full-matrix least-square on F ²					
Data / restraints / parameters	3934 / 0 / 154	3903 / 0 / 172	4777 / 2 / 173	3097 / 0 / 154	3777 / 0 / 181	3871 / 0 / 181
Goodness-of-fit on F²	1.067	1.051	0.936	1.043	1.057	1.023
Final R indices [<i>I</i> > 2σ(<i>I</i>)]	R1 = 0.0327 wR2 = 0.0909	R1 = 0.0315 wR2 = 0.0873	R1 = 0.0246 wR2 = 0.0506	R1 = 0.0391 wR2 = 0.1066	R1 = 0.0328 wR2 = 0.0831	R1 = 0.0257 wR2 = 0.0563
R indices (all data)	R1 = 0.0376 wR2 = 0.0962	R1 = 0.0355 wR2 = 0.0917	R1 = 0.0364 wR2 = 0.0551	R1 = 0.0457 wR2 = 0.1127	R1 = 0.0443 wR2 = 0.0901	R1 = 0.0373 wR2 = 0.0597
Extinction coefficient	0.680 and -0.235	0.436 and -0.264	0.390 and -0.574	0.407 and -0.256	0.357 and -0.334	0.933 and -0.348
Largest diff. peak and hole/e Å⁻³	C ₁₁ H ₈ N ₂ O ₃ S	C ₁₃ H ₁₂ N ₂ O ₃ S	C ₁₁ H ₆ Br ₂ N ₂ O ₃ S	C ₁₁ H ₈ N ₂ O ₄	C ₁₁ H ₈ Cl ₂ N ₂ O ₅	C ₁₁ H ₈ Br ₂ N ₂ O ₅

- [1] (a) C. Reichardt, *Chem. Rev.* **1994**, *94*, 2319–2358; (b) C. Reichardt, T. Welton, in *Solvents and Solvent Effects in Organic Chemistry*, Wiley-VCH, Weinheim, Germany, 4th edn, **2011**, pp. 359–424.
- [2] V. G. Machado, R. I. Stock, C. Reichardt, *Chem. Rev.* **2014**, *114*, 10429–10475.
- [3] K. Dimroth, C. Reichardt, T. Siepmann, F. Bohlmann, *Justus Liebigs Ann.Chem.* **1963**, *661*, 1–37.
- [4] (a) F. Effenberger, F. Würthner, *Angew. Chem. Int. Ed* **1993**, *32*, 719–721; (b) F. Effenberger, F. Wuerthner, F. Steybe, *J. Org. Chem.* **1995**, *60*, 2082–2091.
- [5] (a) L. G. S. Brooker, G. H. Keyes, R. H. Sprague, R. H. VanDyke, E. VanLare, G. VanZandt, F. L. White, *J. Am. Chem. Soc.* **1951**, *73*, 5326–5332; (b) H. G. Benson, J. N. Murrell, *J. Chem. Soc., Faraday Trans. 2* **1972**, *68*, 137–143; (c) A. Botrel, A. le Beuze, P. Jacques, H. Strub, *J. Chem. Soc. Faraday Trans. 2* **1984**, *80*, 1235–1252; (d) P. Jacques, *J. Phys. Chem.* **1986**, *90*, 5535–5539; (e) J. O. Morley, R. M. Morley, R. Docherty, M. H. Charlton, *J. Am. Chem. Soc.* **1997**, *119*, 10192–10202; (f) V. Cavalli, D. C. da Silva, C. Machado, V. G. Machado, V. Soldi, *J. Fluoresc.* **2006**, *16*, 77–86; (g) N. A. Murugan, J. Kongsted, Z. Rinkevicius, H. Ågren, *Phys. Chem. Chem. Phys.* **2011**, *13*, 1290–1292; (h) D. L. Silva, N. A. Murugan, J. Kongsted, H. Ågren, S. Canuto, *J. Phys. Chem. B* **2014**, *118*, 1715–1725; (i) T. Wada, H. Nakano, H. Sato, *J. Chem. Theory Comput.* **2014**, *10*, 4535–4547.
- [6] C. E. A. de Melo, L. G. Nandi, M. Domínguez, M. C. Rezende, V. G. Machado, *J. Phys. Org. Chem.* **2015**, *28*, 250–260.
- [7] (a) S. Dähne, F. Moldenhauer, *Prog. Phys. Org. Chem.* **1985**, *15*, 1–130; (b) W. Rettig, M. L. Dekhtyar, A. I. Tolmachev, V. V. Kurdyukov, *Chem. Heterocycl. Compd.* **2012**, *47*, 1244–1257; (c) W. Rettig, M. Dekhtyar, *Chem. Phys.* **2003**, *293*, 75–90; (d) M. Dekhtyar, W. Rettig, *Phys. Chem. Chem. Phys.* **2001**, *3*, 1602–1610; (e) G. Bourhill, J.-L. Bredas, L.-T. Cheng, S. R. Marder, F. Meyers, J. W. Perry, B. G. Tiemann, *J. Am. Chem. Soc.* **1994**, *116*, 2619–2620;
- [8] R. Letrun, M. Koch, M. L. Dekhtyar, V. V. Kurdyukov, A. I. Tolmachev, W. Rettig, E. Vauthey, *J. Phys. Chem. A* **2013**, *117*, 13112–13126.
- [9] M. C. Rezende, *J. Phys. Org. Chem.*, **2016**, *29*, 460–467.
- [10] (a) L. G. Nandi, F. Facin, V. G. Marini, L. M. Zimmermann, L. A. Giusti, R. d. Silva, G. F. Caramori, V. G. Machado, *J. Org. Chem.* **2012**, *77*, 10668–10679; (b) R. I. Stock, L. G. Nandi, C. R. Nicoletti, A. D. S. Schramm, S. L. Meller, R. S. Heying, D. F. Coimbra, K. F. Andriani, G. F. Caramori, A. J. Bortoluzzi, V. G. Machado, *J. Org. Chem.* **2015**, *80*, 7971–7983; (c) R. I. Stock, C. E. A. de Melo, A. D. S. Schramm, C. R. Nicoletti, A. J. Bortoluzzi, R. da S. Heying, V. G. Machado, M. C. Rezende, *Phys. Chem. Chem. Phys.* **2016**, *18*, 32256–32265.
- [11] R. I. Stock, A. D. S. Schramm, M. C. Rezende, V. G. Machado, *Phys. Chem. Chem. Phys.* **2016**, *18*, 20266–20269.
- [12] S. M. Johnson, S. Connelly, I. A. Wilson, J. W. Kelly, *J. Med. Chem.* **2008**, *51*, 6348–6358.
- [13] (a) J. Jayabharathi, V. Thanikachalam, K. B. Devi, M. V. Perumal, *J. Fluoresc.* **2012**, *22*, 737–744; (b) J. Catalán, V. López, P. Pérez, R. Martín-Villamil, J. G. Rodríguez, *Liebigs Ann.* **1995**, 241–252; (c) J. Catalán, V. López, P. Pérez, *Liebigs Ann.* **1995**, 793–795; (d) J. Catalán, C. Díaz, V. López, P. Pérez, J.-L. G. de Paz, J. G. Rodríguez, *Liebigs Ann.* **1996**, 1785–1794; (e) J. Catalán, *J. Phys. Chem. B* **2009**, *113*, 5951–5960.
- [14] (a) M. J. Kamlet, J. L. M. Abboud, M. H. Abraham, R. W. Taft, *J. Org. Chem.* **1983**, *48*, 2877–2887; (b) Y. Marcus, *Chem. Soc. Rev.* **1993**, *22*, 409–416; (c) M. El-Sayed, H. Müller, G. Rheinwald, H. Lang, S. Spange, *Chem. Mater.* **2003**, *15*, 746–754; (d) C. T. Martins, M. S. Lima, O. A. El Seoud, *J. Org. Chem.* **2006**, *71*, 9068–9079.
- [15] (a) B. S. Furniss, A. J. Hannaford, P. W. G. Smith, A. R. Tatchell, *Vogel's Textbook of Practical Organic Chemistry*, Longman, London, 5th edn, **1989**; (b) D. B. G. Williams, M. Lawton, *J. Org. Chem.* **2010**, *75*, 8351–8354.
- [16] M. Rezende, R. Oñate, M. Domínguez, D. Millán, *Spectrosc. Lett.* **2009**, *42*, 81–86.
- [17] SADABS, APEX2 and SAINT, Bruker AXS Inc.: Madison, WI, **2009**.
- [18] G. Sheldrick, *Acta Crystallogr., Sect. A: Found. Crystallogr.* **2008**, *64*, 112–122.
- [19] (a) A. Spek, *J. Appl. Crystallogr.* **2003**, *36*, 7–13. (b) C. F. Macrae, I. J. Bruno, J. A. Chisholm, P. R. Edgington, P. McCabe, E. Pidcock, L. Rodriguez-Monge, R. Taylor, J. van de Streek and P. A. Wood, *J. Appl. Crystallogr.* **2008**, *41*, 466–470.
- [20] B. Hess, C. Kutzner, D. van der Spoel, E. Lindahl, *J. Chem. Theory Comput.* **2008**, *4*, 435–447.
- [21] W. L. Jorgensen, J. Tirado-Rives, *J. Am. Chem. Soc.* **1988**, *6*, 1657–1666.
- [22] H. J. C. Berendsen, J. R. Grigera, T. P. Straatsma, *J. Phys. Chem.* **1987**, *91*, 6269–6271.
- [23] C. M. Breneman, K. B. Wiberg, *J. Comput. Chem.* **1990**, *11*, 361–373.
- [24] M. J. Frisch, G. W. Trucks, H. B. Schlegel, G. E. Scuseria, M. A. Robb, J. R. Cheeseman, G. Scalmani, V. Barone, G. A. Petersson, H. Nakatsuji, X. Li, M. Caricato, A. Marenich, J. Bloino, B. G. Janesko, R. Gomperts, B. Mennucci, H. P. Hratchian, J. V. Ortiz, A. F. Izmaylov, J. L. Sonnenberg, D. Williams-Young, F. Ding, F. Lipparini, F. Egidi, J. Goings, B. Peng, A. Petrone, T. Henderson, D. Ranasinghe, V. G. Zakrzewski, J. Gao, N. Rega, G. Zheng, W. Liang, M. Hada, M. Ehara, K. Toyota, R. Fukuda, J. Hasegawa, M. Ishida, T. Nakajima, Y. Honda, O. Kitao, H. Nakai, T. Vreven, K. Throssell, J. A. Montgomery, Jr., J. E. Peralta, F. Ogliaro, M. Bearpark, J. J. Heyd, E. Brothers, K. N. Kudin, V. N. Staroverov, T. Keith, R. Kobayashi, J. Normand, K. Raghavachari, A. Rendell, J. C. Burant, S. S. Iyengar, J. Tomasi, M. Cossi, J. M. Millam, M. Klene, C. Adamo, R. Cammi, J. W. Ochterski, R. L. Martin, K. Morokuma, O. Farkas, J. B. Foresman, and D. J. Fox. *Gaussian 09, Revision C.01*; Gaussian, Inc., Wallingford CT **2016**.
- [25] (a) A. D. J. Becke, *J. Phys. Chem.* **1993**, *98*, 5648–5652; (b) C. Lee, W. Yang, R. G. Parr, *Phys. Rev. B: Condens. Matter* **1988**, *37*, 785–789; (c) S. H. Vosko, L. Wilk, M. Nusair, *Can. J. Phys.* **1980**, *58*, 1200–1211; (d) P. J. Stephens, F. J. Devlin, C. F. Chabalowski, M. J. Frisch, *J. Phys. Chem.* **1994**, *98*, 11623–11627.
- [26] (a) V. A. Rassolov, J. A. Pople, M. A. Ratner, T. L. Windus, *J. Chem. Phys.* **1998**, *109*, 1223–1229; (b) V. A. Rassolov, M. A. Ratner, J. A. Pople, P. C. Redfern, L. A. Curtiss, *J. Comput. Chem.* **2001**, *22*, 976–998.

Compounds with phenols as electron-donating groups and 5-nitrothiophen-2-yl or 5-nitrofuran-2-yl acceptor moieties in their molecular structures were synthesized. The crystalline structures of six compounds were obtained. Their corresponding phenolate dyes were studied in 29 solvents and the data showed that in all cases a reverse solvatochromism occurred. The results were explained in terms of the ability of the medium to stabilize the electronic ground and excited states of the probes to different extents.



Carlos E. A. de Melo,^[a] Celso R. Nicoleti,^[a] Marcos C. Rezende,^[b] Adailton J. Bortoluzzi,^[a] Renata da S. Heying,^[a] Robson da S. Oliboni,^[c] Giovanni F. Caramori,^[a] Vanderlei G. Machado^[a,*]

Page No. – Page No.

Reverse solvatochromism of imine dyes comprised of 5-nitrofuran-2-yl or 5-nitrothiophen-2-yl as electron acceptor and phenolate as electron donor